

1 LIP - Laboratório de Instrumentação e Física Experimental de Partículas
2



3 Jets and charged hadrons in heavy ion collisions with the
4 ATLAS detector *

5 HELENA SANTOS, ON BEHALF OF THE ATLAS COLLABORATION

6 Ultrarelativistic heavy ion collisions at the LHC produce the Quark
7 Gluon Plasma. Jets are a useful probe to study this state of matter since
8 they are produced at the early stages of the collisions and are expected to
9 be modified as propagating through the medium. One observable is the
10 energy loss lowering the jet yields at a given transverse momentum. Other
11 observables are the modification of the dijet momentum balance and the
12 modification of fragmentation functions. A phenomenon strictly correlated
13 to the jet energy loss is the modification of the charged-hadron momentum
14 spectrum. The large new Pb+Pb data sample collected by ATLAS in Run
15 2 allows precision measurements of these observables in a wide transverse
16 momentum range and in different centrality and rapidity intervals.

17 PACS numbers: 12.38.Mh,13.87.Ce,13.87.Fh

18 **1. Introduction**

19 A wide research program is ongoing at the Large Hadron Collider with
20 the aim of studying the properties of QCD matter at extreme temperatures
21 and densities. Jets produced in ultra-relativistic heavy ion collisions consti-
22 tute a golden probe of such a state of matter. The hard scattered quarks and
23 gluons emerged from these collisions evolve as parton showers that propa-
24 gate through the hot and dense medium. Constituents of the parton showers
25 emit medium-induced gluon radiation and, as a consequence, the resulting
26 jet loses energy, a phenomenon commonly termed as jet quenching [1]. Jets
27 produced in heavy ion collisions are thus expected to be suppressed at a
28 given p_T , relatively to a sample produced in pp collisions. Their internal
29 structure is also expected to be modified. The large acceptance and high
30 granularity of the ATLAS detector [2] is well suited to study these phenom-
31 ena. Results shown in this conference used data produced in Pb+Pb and
32 pp collisions at the center of mass energies of 2.76 TeV and 5.02 TeV. The

* This work was supported in part by FCT under the contract Project IF/01586/2014/CP1248/CT0003

33 centrality of the Pb+Pb collisions is estimated using the total transverse
 34 energy deposited in the forward calorimeters (FCal, $3.2 \leq |\eta| < 4.9$) and
 35 compared to a Glauber Monte Carlo model [3], convoluted with pp data
 36 taken at the same beam energy. The $\sum E_T^{\text{FCal}}$ distribution is then divided
 37 into percentiles of the total inelastic cross-section for Pb+Pb collisions. Jets
 38 are reconstructed using calorimeter “towers” as input signals to the anti- k_t
 39 algorithm, with jet radius parameter size $R = 0.4$. The underlying event
 40 is estimated and subtracted event-by-event in each calorimeter layer and
 41 strip of pseudorapidity after excluding regions subtending jet candidates
 42 and corrected for flow modulation.

43 2. Results

44 The nuclear modification factor R_{AA} , defined as the ratio of normalized
 45 yields in Pb+Pb and pp collision systems, is used to compare the inclusive
 46 transverse momentum distributions measured in the two collision systems:

$$R_{\text{AA}} \equiv \frac{(1/N_{\text{evt}}) \left. \frac{d^2 N_{\text{jet}}^{\text{PbPb}}}{dp_T dy} \right|_{\text{cent}}}{\langle T_{\text{AA}} \rangle \frac{d^2 \sigma_{\text{jet}}^{\text{pp}}}{dp_T dy}}, \quad (1)$$

47 where $\langle T_{\text{AA}} \rangle$ stands for the geometric enhancement of per-collision nucleon-
 48 nucleon luminosity and N_{evt} is the total number of Pb+Pb collisions within
 49 a chosen centrality interval. The jet yields, unfolded for detector resolution,
 50 bin-to-bin migration and reconstruction inefficiency, are shown in Fig.1.
 51 Jets are suppressed increasingly with collisions centrality, reaching a factor
 52 of two in central collisions (0–10%), while showing little dependence on jet
 53 transverse momentum and rapidity [4]. These measurements confirm the
 54 expectations on the reduction of the jet yields at a given transverse energy
 55 due to the interaction of partons in the quark gluon plasma [1].

56 A complementary observable to jet production is the measurement of
 57 charged particle spectra, as these contribute to the understanding of jet
 58 energy loss mechanisms. Tracks are reconstructed using the ATLAS in-
 59 ner detector system in the pseudorapidity range $|\eta| < 2.5$ and over the
 60 full azimuthal acceptance. Corrections to measured p_T spectra, like fake
 61 tracks, bin-to-bin migration, and reconstruction inefficiency are estimated
 62 from Monte Carlo simulations. The charged hadron R_{AA} as a function of
 63 p_T is shown in Fig.2. A characteristic p_T shape, which becomes more pro-
 64 nounced with increasing centrality, is observed. The R_{AA} distributions first
 65 increase reaching a local maximum at $p_T < 2$ GeV, a feature commonly asso-
 66 ciated with the Cronin effect [5], i.e. hardening of the p_T spectrum in heavy
 67 ion collisions relative to pp collisions, often understood to be due to multiple
 68 scattering of partons. At higher p_T the R_{AA} decreases reaching a minimum

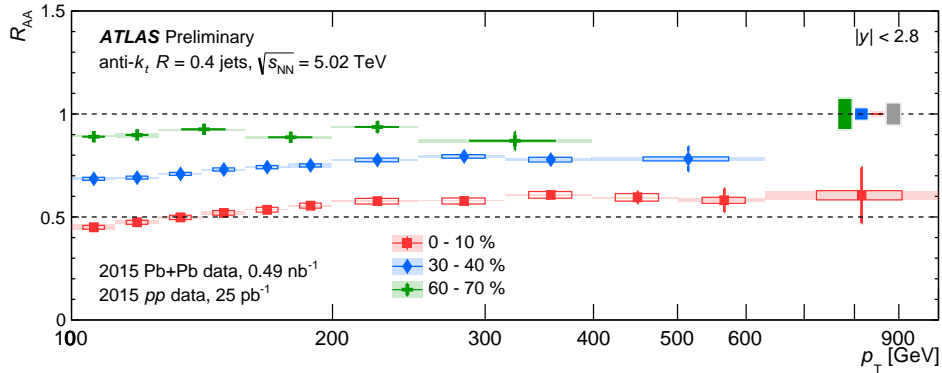


Fig. 1. The R_{AA} as a function of jet p_T for jets with $|y| < 2.8$ for three centrality bins. The error bars represent statistical uncertainties, the shaded boxes around the data points represent correlated systematic uncertainties, open boxes represent uncorrelated systematic uncertainties. The colored shaded boxes at unity represent $\langle T_{AA} \rangle$ uncertainties and the gray shaded box represents the uncertainty on pp luminosity. The horizontal width on the shaded boxes represents the width of the p_T interval and the horizontal widths on the open boxes are arbitrary for better visibility [4].

69 at $p_T = 7$ GeV. The rate of charged particles is noticeably suppressed even
 70 in the 60–80% centrality interval but the suppression is strongest in the
 71 most central 0–5% collisions. Above 7 GeV, the R_{AA} generally increase
 72 with increasing p_T up to 60 GeV, after which the slope changes. Details of
 73 this analysis can be found in [6].

74 Jet fragmentation functions are measured aiming a deeper understand-
 75 ing of the jet energy loss nature and constraining jet quenching models. The
 76 jet structure is probed in the p_T range from 100 to 398 GeV, using tracks
 77 with $p_T > 1$ GeV. The fragmentation functions, defined as $D[z(p_T)] =$
 78 $(1/N_{\text{jet}}) dN_{\text{ch}} / dz(p_T)$, are studied as a function of the longitudinal momen-
 79 tum fraction, $z = p_T^{\text{ch}} / p_T^{\text{jet}} \cos \Delta R$, and track p_T , where p_T^{ch} stands for the
 80 transverse momentum of a charged particle and ΔR is the distance between
 81 the charged particle and the jet axis. The $D(z)$ and $D(p_T)$ distributions
 82 are background subtracted, corrected for reconstruction inefficiency and un-
 83 folded with a 2D Bayesian method. Figure 3 shows the modification of the
 84 fragmentation functions, assessed with $R_{D(z)} = D(z)|_{\text{Pb+Pb}} / D(z)|_{\text{pp}}$ in dif-
 85 ferent ranges of rapidity. An enhancement at low z , up to 0.03, and at z
 86 larger than 0.2, mainly at mid-rapidity, is observed in central collisions. The
 87 range $0.03 < z < 0.2$ shows a clear depletion. The enhancement of fragment
 88 yields at low z is consistent with an interpretation in which the energy lost

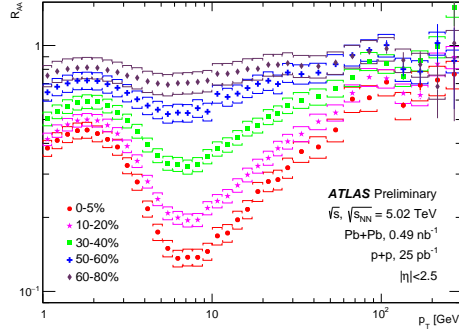


Fig. 2. Nuclear modification factor R_{AA} as a function of p_T for charged hadrons measured in Pb+Pb collisions at $\sqrt{s_{NN}}=5.02$ TeV for five centrality intervals: 0-5%, 10-20%, 30-40%, 50-60% and 60-80%. Bars represent the statistical uncertainties and brackets represent the systematic uncertainties [6].

89 by partons is transferred predominantly to soft particles [7]. Details on this
 90 analysis can be found in [8].

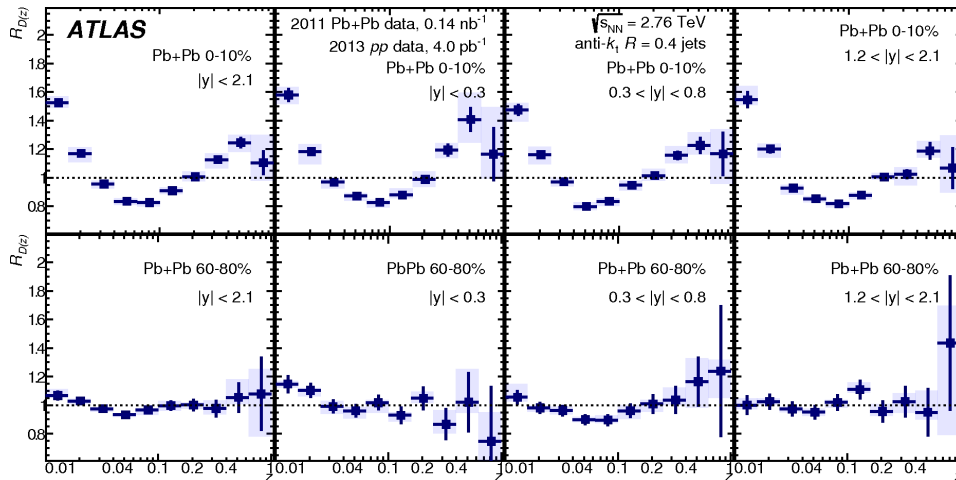


Fig. 3. The ratio $R_{D(z)}$ of unfolded $D(z)$ distributions measured in heavy-ion collisions to unfolded $D(z)$ distributions measured in pp collisions. The $R_{D(z)}$ distributions shown here are evaluated in two different centrality bins (rows) and four different selections in jet rapidity (columns). The error bars on the data points indicate statistical uncertainties while the shaded bands indicate systematic uncertainties [8].

91

92 The first indication of jet quenching was given by the observation of

93 large asymmetrical dijet events [9]. Dijets probe differences in the two par-
 94 ton showers since in most of the cases the interaction of the two outgoing
 95 partons in the quark gluon plasma is not identical. A new analysis has
 96 been performed using $140 \mu b^{-1}$ of Pb+Pb data taken at $\sqrt{s_{NN}}=2.76$ TeV
 97 and benefiting from a deeper understanding of the underlying event and
 98 analysis conditions. Figure 4 shows the distribution of dijets produced in
 99 Pb+Pb and pp collisions as a function of x_J , the ratio between the trans-
 100 verse momenta of the two leading jets. The measured distributions are
 101 unfolded to account for the effects of experimental resolution and inefficien-
 102 cies on the two-dimensional (p_{T_1}, p_{T_2}) distributions and then projected into
 103 bins of fixed ratio $x_J = p_{T_1}/p_{T_2}$. The observation of large asymmetric di-
 104 jets in central collisions is striking. The distributions in the two colliding
 105 systems become increasingly similar with decreasing centrality. Interesting
 106 is the study of the variation of the dijet asymmetry with the p_T of the
 107 leading jet. A modification in the asymmetry in Pb+Pb collisions as the
 108 p_T of the leading jet increases is observed, indicating that higher transverse
 109 momentum jets lose less energy and so tend to be more balanced. This
 110 feature is particularly evident for transverse momentum greater than 200
 111 GeV. Details on this analysis can be found in [10].

112 3. Conclusions

113 Inclusive jets yields are found to be suppressed with collisions centrality,
 114 reaching a factor of two in central collisions, while showing little dependence
 115 on jet transverse momentum and rapidity. In contrast, the nuclear modifi-
 116 cation factor of charged hadrons shows a striking non-flat p_T shape which
 117 becomes more pronounced with increasing centrality. The jet structure is
 118 modified: in central collisions there is an enhancement of particles at low and
 119 high z , while a suppression at intermediate z is observed. The p_T balance of
 120 dijets produced in Pb+Pb collisions is increasingly asymmetric when com-
 121 pared to the pp results as the centrality of the collisions increases. At larger
 122 values of p_{T_1} the x_J distributions are observed to narrow and the differences
 123 between the distributions in central Pb+Pb and pp collisions become much
 124 smaller.

REFERENCES

- 125 [1] J.-P. Blaizot and Y. Mehtar-Tani, *J. Mod. Phys.* **E24** (2015) 1530012 (and
 126 references therein). arXiv: 1503.05958 [hep-ph]
 127 [2] ATLAS Collaboration, *JINST* **3** (2008) S08003.
 128 [3] M. L. Miller, K. Reygers, S. J. Sanders, and P. Steinberg, *Ann. Rev. Nucl.*
 129 *Part. Sci.* **57** (2007) 205.

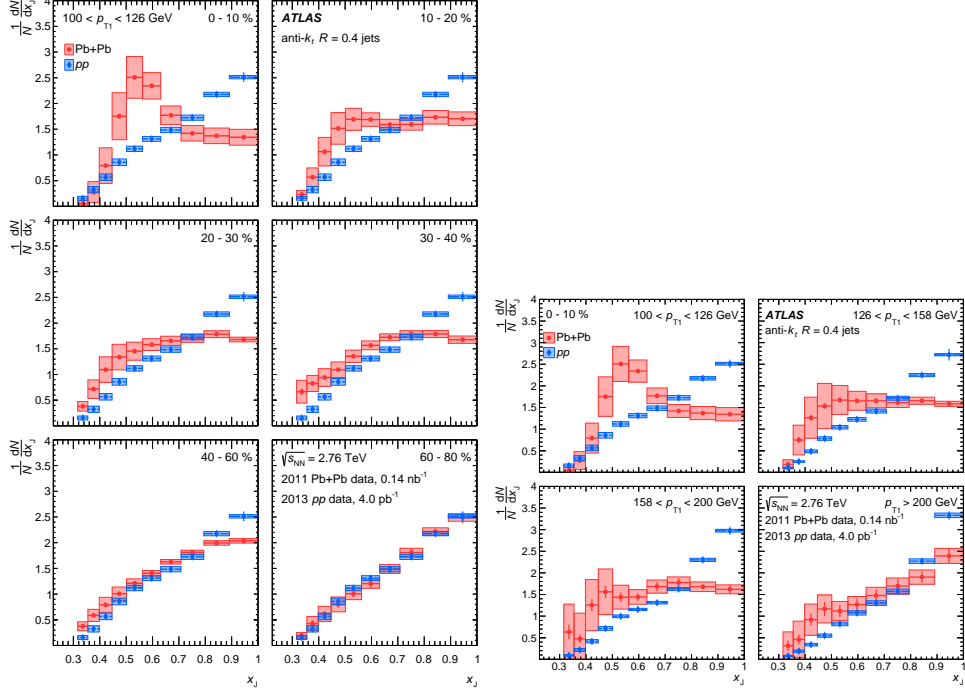


Fig. 4. Left: The $(1/N)dN/dx_J$ distributions for jet pairs with $100 < p_{T_1} < 126$ GeV for different collision centralities and for $R=0.4$ jets. The Pb+Pb data are shown in red circles, while the pp distribution is shown for comparison in blue diamonds and is the same in all panels. Right: The $(1/N)dN/dx_J$ distributions with different selections on p_{T_1} , shown for the 0–10% centrality interval (red circles) and for pp (blue diamonds). In both panels the statistical uncertainties are indicated by the error bars while systematic uncertainties are shown with shaded boxes [10].

- 130 [4] ATLAS Collaboration, *ATLAS-CONF-2017-009*.
 131 <http://cds.cern.ch/record/2244820>
- 132 [5] J. W. Cronin et al., *Phys. Rev. D* **11** (1975) 3105.
- 133 [6] ATLAS Collaboration, *ATLAS-CONF-2017-012*.
 134 <http://cds.cern.ch/record/2244824>
- 135 [7] CMS Collaboration, *Phys. Rev. C* **84** (2011) 024906. arXiv: 1102.1957 [nucl-
 136 ex].
- 137 [8] ATLAS Collaboration, *Eur. Phys. J C* **77** (2017) 379. arXiv:1702.00674 [hep-
 138 ex]
- 139 [9] ATLAS Collaboration, *Phys. Rev. Lett.* **105** (2010) 252303. arXiv:1011.6182
 140 [hep-ex]
- 141 [10] ATLAS Collaboration, submitted to *Phys. Lett. B.*. arXiv:1706.09363 [hep-ex]